New Criterion For The Liquefaction Resistance Under Strain-Controlled Multi-Directional Cyclic Shear

H. Matsuda, T.T. Nhan, R. Ishikura & T. Inazawa
Yamaguchi University, Ube, Japan

P.H. Andre
Brawijaya University, Malang, Indonesia

SUMMARY:
This paper is to investigate the effect of cyclic shear direction on the liquefaction characteristics of saturated granular materials such as effective vertical stress reduction, several series of multi-directional cyclic simple shear test were performed for granular materials including the crushable and non-crushable soils under the strain-controlled condition. It is shown from the test results that the reduction of effective vertical stress is affected by cyclic shear direction. However, this effect is negligible when shear strain amplitude is larger than 0.3%. The reduction of effective vertical stress is a function of cumulative shear strain G^*, which is newly defined as the accumulation of shear strain increment. The relationships between the cumulative shear strain and the shear strain amplitude were derived to show a criterion for the liquefaction resistance. The liquefaction of soil specimen under earthquake-induced strain histories can be evaluated using this criterion.

Keywords: Liquefaction; granular material; effective stress

1. INTRODUCTION

In cyclic loading situations, granular materials are believed to be less stable compared with cohesive soils and consequently many studies on dynamic properties have been carried out for cohesionless soils. Mostly, however, they focus only on uni-directional cyclic shear. Meanwhile, it is known that during earthquake, soil layers are subjected to multi-directional cyclic shear with different strain amplitudes and frequencies. Fig. 1.1 shows the time histories and orbits of shear strain calculated based on the records at Hyogo-ken Nanbu Earthquake 1995, in which multi-directional strain histories of the ground are shown.

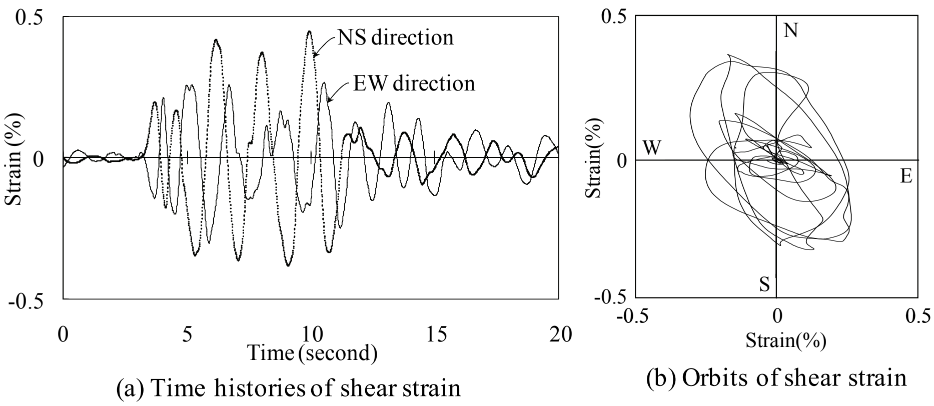

Figure 1.1. Time histories and orbits of shear strain at Hyogo-ken Nanbu Earthquake 1995

Several studies have been carried out to investigate the effective stress change of sandy soils induced by multi-directional cyclic shear. By the multi-directional shaking tests, Pyke et al. (1975) stated that the settlement produced by the multi-directional shaking tests is larger than those in uni-directional ones. By using the simple shear test device under the application of irregular load, Ishihara and Yoshimine (1992) showed the maximum shear strain during undrained cyclic loading is the most appropriate index parameter affecting the post-earthquake settlement in sand deposits. Later, Matsuda et al. (2004; 2011) investigated the effects of cyclic shear direction and cyclic shear strain amplitude on the properties of saturated granular materials by using the multi-directional cyclic simple shear test apparatus and concluded that the vertical effective stress reduction during cyclic loading and the post-cyclic settlement induced by multi-directional shear are larger than those induced by uni-directional cyclic shear. In addition, Matsuda et al. (2011) recently evaluated the relationships between post-cyclic settlement and effective stress reduction of granular materials by using cumulative shear strain and resultant shear strain. The authors then proposed the estimation method of effective stress change by using these two shear strain parameters.

By using a multi-directional cyclic simple shear test apparatus, Toyoura sand, which is considered as non-crushable soil and granulated blast furnace slag (hereinafter referred to as GBFS), which is considered as crushable soil were tested under strain-controlled uniform cyclic shear at different shear strain amplitudes, phase differences and number of cycles, and under irregular cyclic shear at different shear strain amplitudes. The effect of cyclic shear direction on the liquefaction resistance in terms of effective vertical stress reduction was investigated and the relations between cumulative shear strain G^* and shear strain amplitude γ for the liquefaction was obtained to develop a criterion for liquefaction resistance under the regular cyclic shear. Finally, the practical applicability of this criterion was confirmed.

2. APPARATUS, SPECIMENS AND TEST PROCEDURES

Fig. 2.1 shows outline of the apparatus. This apparatus can give any types of cyclic displacement at the centre of the bottom of specimen from two perpendicular directions. A predetermined vertical stress can be applied to the specimen by the electro-controlled aero-servo system. The shear box is the Kjellman type in which the specimens were enclosed in a rubber membrane. The flank of the membrane-enclosed specimen was surrounded by a stack of 10 acrylic rings. Each acrylic ring has 75.8 mm in inside diameter and 2 mm in thickness. From this arrangement, the specimen is prevented from the radial deformation but permitted the shear deformation during cyclic simple shear.

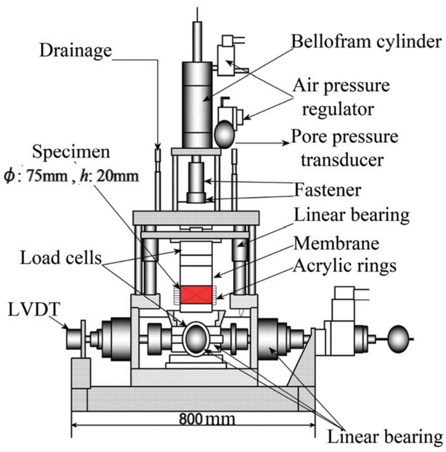

Figure 2.1. Outline of the test device

The soils used in this study were Toyoura sand and GBFS. The particle size distribution curves and the physical properties of these materials are shown in Fig. 2.2 and Table 2.1, respectively. It is seen that GBFS has almost the similar unit weight of soil grains as natural sand. GBFS is mainly used to produce blast furnace cement in Japan. As an alternative material, GBFS is considered to be one of promising materials in geotechnical engineering, because it has particular properties such as light weight, high shear strength and high permeability. As compared with natural sand, GBFS is easy to be crushed by the applied load and under the multi-directional cyclic shear, the amount of particle crush and the settlement are larger than those induced by uni-directional cyclic shear (Matsuda et al., 2006). The applicability of GBFS as an earthquake-resistant material and light-weight embankments has also been investigated and it is clarified that its shear strength increases with time by its hydraulic property under ordinary natural wet condition (Matsuda et al., 2008).

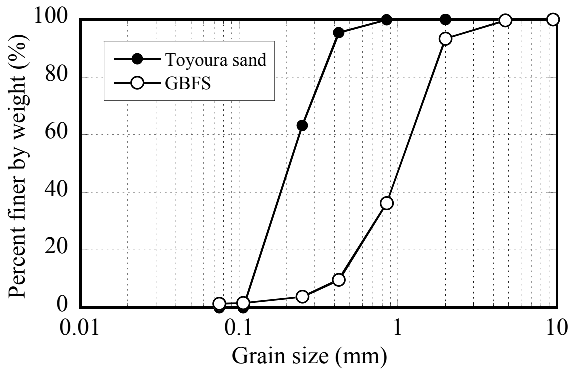

Figure 2.2. Grain size distribution of samples

Table 2.1. Physical properties of sample

Properties	Toyoura sand	GBFS
Density of soil particles ρ_s (g/cm^3)	2.637	2.643
Maximum void ratio e_{max}	0.991	1.510
Minimum void ratio e_{min}	0.630	1.033

In order to prepare the soil specimen, Toyoura sand and GBFS were saturated in de-aired water. The soil sample was then poured into the shear box with a predetermined relative density. Thereafter, the specimen was consolidated for 15 minutes under the vertical stress σ_v' = 49 kPa. After preconsolidation, the specimen has the size of 75 mm in diameter and about 20 mm in height which was then subjected to cyclic shear under undrained conditions for predetermined number of cycles, shear strain amplitude and phase difference. During cyclic shear, the vertical displacement was kept constant to satisfy the undrained condition.

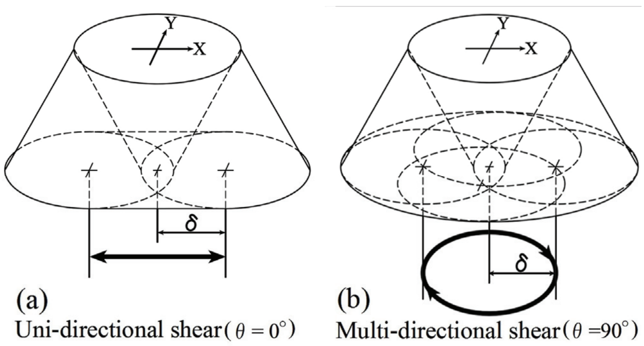

Figure 2.3. Typical deformations of specimen

Experiments in this study were performed under the condition of strain-controlled uni-directional and multi-directional cyclic simple shears. Toyoura sand and GBFS were tested for three relative densities of Dr = 50%, 70% and 90% referring to loose, medium and high density, respectively. The shear strain amplitude was set in the range from γ = 0.1% to 2.0% and the number of cycles was fixed in a range from 1 to 150. The wave form of the cyclic shear strain was sinusoidal with the period 2 s. Fig. 2.3 shows typical deformations of specimen, conceptually. The shear strain amplitude γ is defined as a ratio of the maximum horizontal displacement δ to the initial height of the specimen. In addition, several multi-directional cyclic shear tests were carried out under the irregular shear strain cycles with the different maximum shear strain amplitudes, which was derived from the time histories of acceleration recorded at Hyogo-ken Nanbu Eathquake 1995.

Typical records of uniform cyclic shear strain and the respective orbits at phase difference $\theta = 0^0$, 45^0 and 90^0 are shown in Figs. 2.4 and 2.5, respectively, in which the shear strain amplitude was set as 1.0%. In uni-directional cyclic shear test, the shear strain was applied to the specimen only in one direction (in this case: *X* direction (Fig. 2.4a)) or in both *X* and *Y* directions with no phase difference ($\theta = 0^0$), and so the orbit of cyclic shear strain forms linear lines (Fig. 2.5). In multi-directional cyclic shear tests, the shear strain was simultaneously applied to *X* direction (γ_x) and *Y* (γ_y) direction which are perpendicular to each other under the same shear strain amplitude but at different phase differences (Figs. 2.4b and c). Then the orbit forms from elliptical lines ($\theta = 45^0$) to circle lines ($\theta = 90^0$) which is commonly known as gyratory cyclic shear condition (Fig. 2.5). The effects of phase difference on the formation of the orbit can be seen in Fig. 2.5.

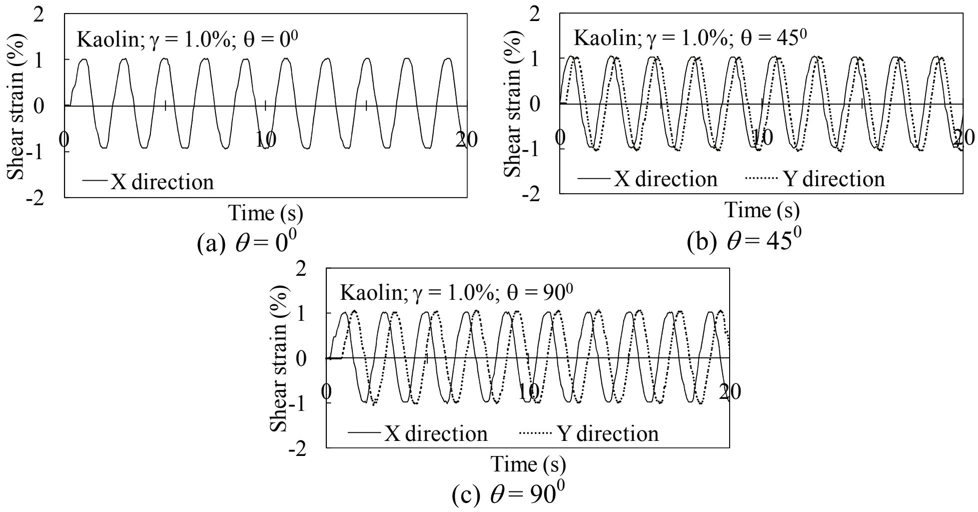

Figure 2.4. Time histories of cyclic shear strain at $\gamma = 1.0\%$ under various phase differences

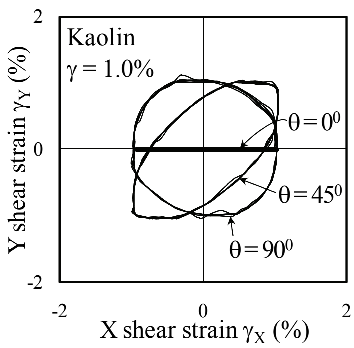

Figure 2.5. Orbits of shear strain at $\gamma = 1.0\%$ under various phase differences

3. TEST RESULTS AND DISCUSSIONS

3.1. Change in Effective Stress during Cyclic Shear

Typical records of effective vertical stress decrease on Toyoura sand by the multi-directional shearing under various phase differences are shown Figs. 3.1(a) and (b) for shear strain amplitude $\gamma = 0.1\%$ and 1.0%, respectively. In general, effective vertical stress decreases with the number of strain cycles. When effective vertical stress comes to zero, then it refers to totally a loss of shear strength of soils or liquefaction condition has been reached. It can be observed that effective vertical stress reduction in the case of multi-directional shear is larger than that of uni-directional shear. In Fig. 3.1(b), larger shear strain amplitude implicates the sudden decrease of effective vertical stress and mostly, the number of cycles required to reach liquefaction was less than 5, regardless of the directions of cyclic shear. These results show that shear strain amplitude and phase difference have significant effects on the liquefaction resistance of granular materials.

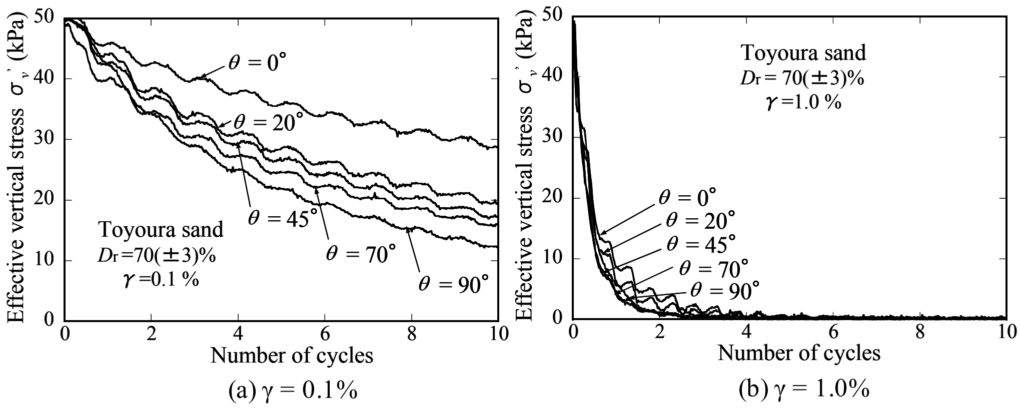

Figure 3.1. Effective stress change versus number of cycles

The relations of the effective stress reduction ratio induced by uni-directional and multi-directional shears versus cumulative shear strain G^* which is defined as the length along the shear strain path during cyclic shear (Fukutake and Matsuoka, 1989) are shown in Figs. 3.2(a) and (b) for $\gamma = 0.1\%$ and 0.3%, respectively. G^* is defined as follows:

$$G^* = \sum \Delta G^* = \sum \sqrt{\Delta\gamma_x^2 + \Delta\gamma_y^2} \tag{3.1}$$

where $\Delta\gamma_x$ and $\Delta\gamma_y$ are shear strain increments at X and Y directions, respectively.

It is observed in Figs. 3.2(a) and (b) that the effective stress reduction ratio increases as a function of cumulative shear strain at each phase difference. Especially, in Fig. 3.2(b), the dependency of $|\Delta\sigma'_v/\sigma'_{vo}|$ on G^* is negligible for all various phase differences. This means that at larger shear strain amplitude, the phase difference has little influence on the effective stress reduction. Also in these figures, the threshold cumulative shear strain G^*_{min} under which no reduction of effective vertical stress occurs is $G^*_{min} = 0.1\%$ for different shear strain amplitudes.

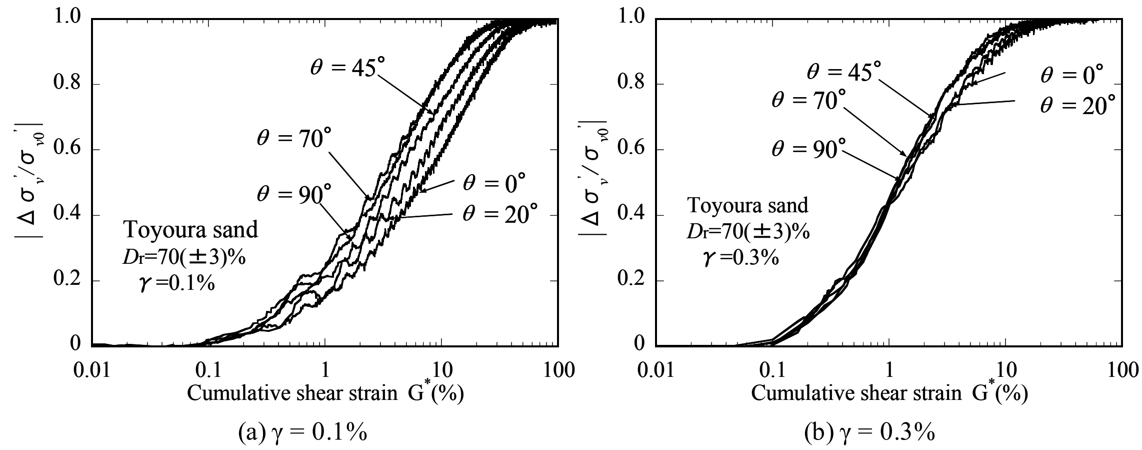

Figure 3.2. Effective stress reduction ratio versus cumulative shear strain

Matsuda et al. (2011) proposed an equation to express the relations between the effective stress reduction ratio $|\Delta\sigma'_v/\sigma'_{vo}|$ and the cumulative shear strain for granular materials subjected to multi-directional shear, as follows:

$$\left|\frac{\Delta\sigma'_v}{\sigma'_{v0}}\right| = \frac{G^*}{\alpha + \beta \bullet G^*} \tag{3.2}$$

where $\Delta\sigma'_v$ represents the decrease of effective vertical stress, σ'_{vo} denotes the initial effective vertical stress. In Eqn. 3.2, α and β are defined as α=$A\gamma^m$ and β=$\gamma/(B+C\gamma)$ in which A, B, C and m are the experimental parameters and can be determined by the curve-fitting methods. These experimental constants A, B, C and m obtained for Toyoura sand and GBFS are shown Table 3.1.

Table 3.1. Coefficient of A, B, C and m.

Material	Dr (%)	A	B	C	m
Toyoura sand	50	1.00	0.01	0.96	-0.40
	70	1.20	0.02	1.05	0.55
	90	1.90	0.02	0.98	-0.70
GBFS	50	2.30	-0.04	1.00	-0.40
	70	2.40	-0.05	1.00	-0.42
	90	2.70	0.05	1.00	0.32

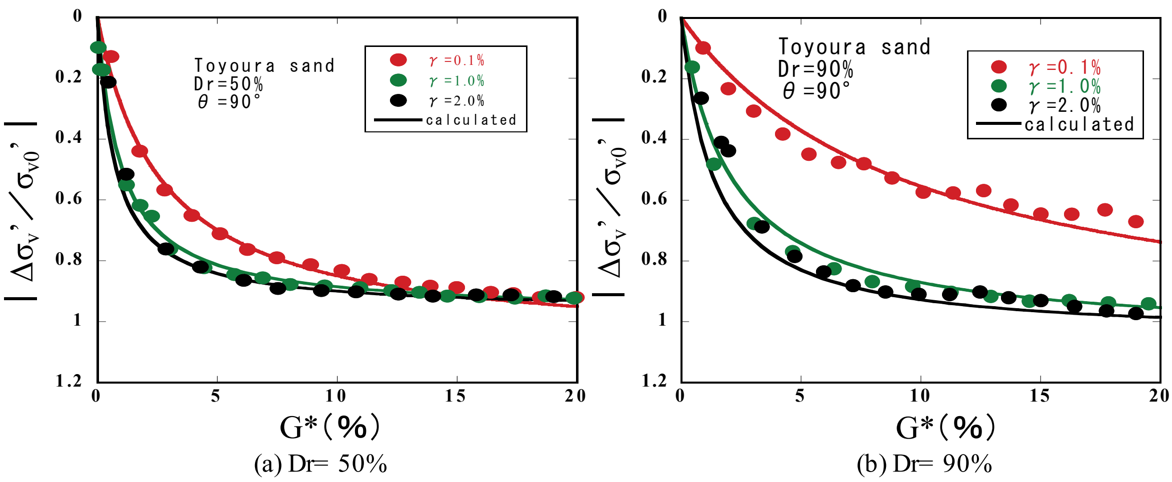

Figure 3.3. Comparison between the observed and calculated results for effective stress reduction ratio induced by multi-directional cyclic shear (θ= 90^0) on Toyoura sand at different relative densities

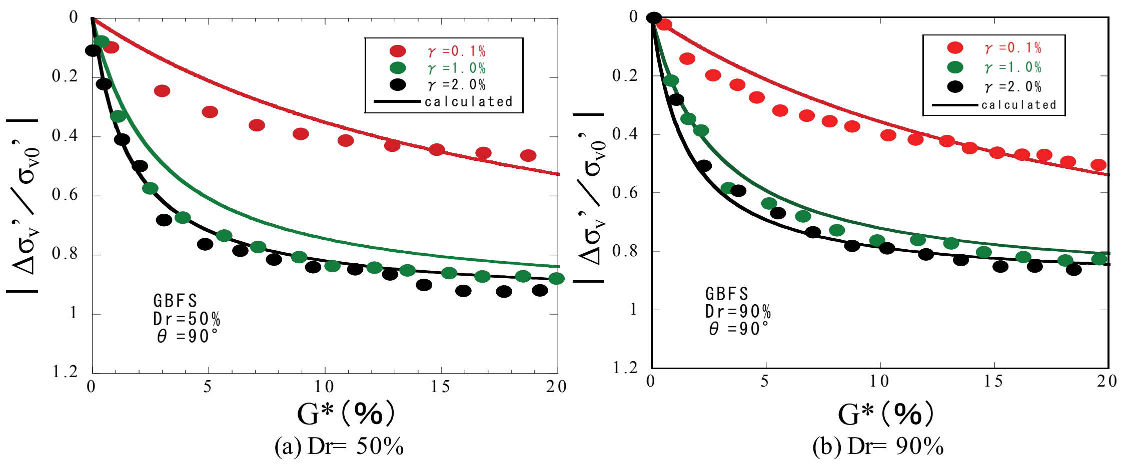

Figure 3.4. Comparison between the observed and calculated results for effective stress reduction ratio induced by multi-directional cyclic shear (θ= 90^0) on GBFS at different relative densities

The comparisons between the observed and calculated results for the effective stress reduction ratio induced by multi-directional shear at $\theta = 90°$, the shear strain amplitude $\gamma = 0.1\%$, 1.0% and 2.0%, and the relative density Dr = 50% and 90% are shown in Figs. 3.3 and 3.4 for Toyoura sand and GBFS, respectively. Symbols in these figures show observed results and solid curves correspond to calculated ones by using Eqn. 3.2 in which constants A, B, C and m in Table 3.1 are used. The calculated results agree with the observed ones reasonably. By comparing test results under different relative densities, it is apparent that at the dense specimens (Dr = 90%) effective stress decreases with a slower rate than that of specimens having lower density. When comparing the materials, it is seen that GBFS shows smaller effective stress reduction ratio than that of Toyoura sand. These facts indicate that GBFS has higher shear strength as well as higher liquefaction resistance than Toyoura sand.

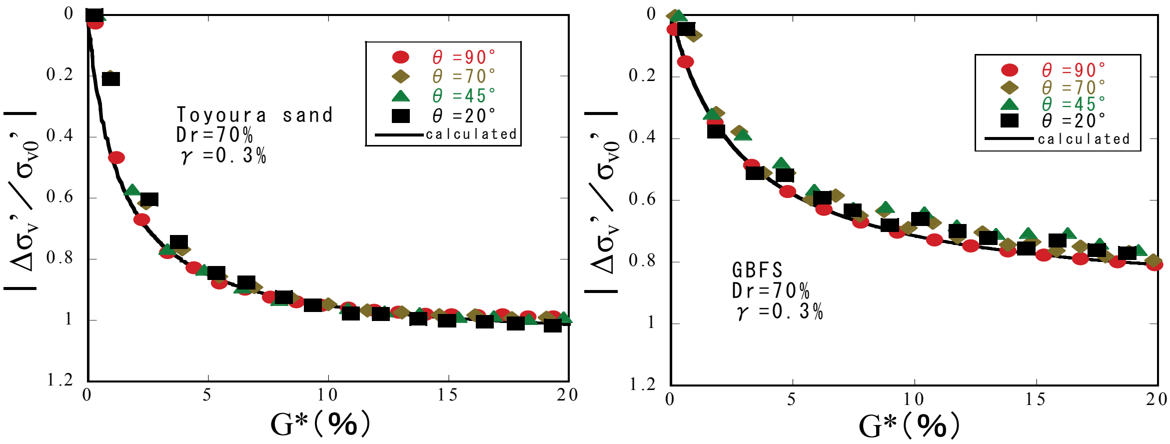

(a) Toyoura sand (b) GBFS

Figure 3.5. Comparisons between the observed and calculated results for effective stress reduction ratio on Toyoura sand and GBFS under multi-directional cyclic shear at various phase differences

The relations of effective stress reduction ratio induced by multi-directional cyclic shear at various phase differences versus cumulative shear strain are shown in Figs. 3.5(a) and (b) for Toyoura sand and GBFS, respectively. The relative density is Dr = 70% and the shear strain amplitude is $\gamma = 0.3\%$. Symbols in these figures show experimental results and solid curves correspond to calculated ones by using Eqn. 3.2 in which constants A, B, C and m in Table 3.1 are used. The calculated results agree well with the observed data for various phase differences. By considering the effect of phase difference, it has been concluded that when shear strain amplitude is relatively large ($\gamma > 0.3\%$), the effective stress reduction ratio is not influenced by the variation of phase difference. Figs. 3.3 to 3.5 indicate that the effective stress reduction ratio estimated in such a way is applicable for various relative densities and phase differences, at least for shear strain amplitude γ larger than 0.3%.

3.2. A Criterion for Liquefaction Resistance

The relations between the number of cycles for liquefaction under various phase differences versus shear strain amplitude are shown in Fig. 3.6, for Toyoura sand. For the same shear strain amplitude, as the phase difference increases, the number of cycles to the liquefaction decreases, which indicates that multi-directional shearing reduces the liquefaction resistance of granular soils. Moreover, it is seen that when the specimen subjected to shear strain amplitude larger than 2%, a very few number of cycles can initiate liquefaction. In this case, it is difficult to obtain the number of cycles to liquefaction under such a condition. Meanwhile, in Figs. 3.2(a) and (b), the values of cumulative shear strains can be clearly measured from the time when the cyclic shear starts and until the occurrence of liquefaction. Thus the application of cumulative shear strain to find the liquefaction condition is more accurate in very short duration of cyclic shear.

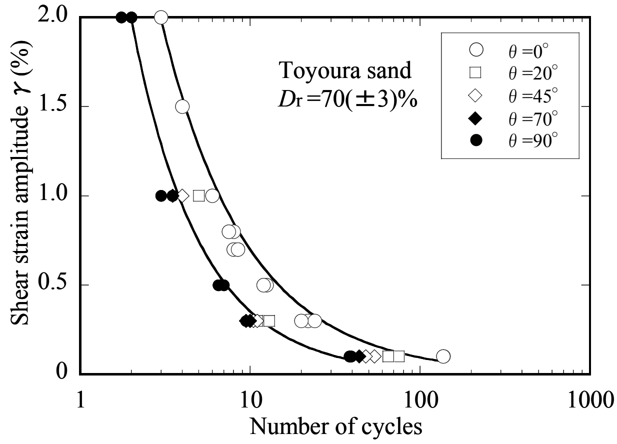

Figure 3.6. Relationship between the number of cycles and shear strain amplitude required for liquefaction

Therefore, it is more useful to plot the relations between cumulative shear strain and shear strain amplitude to show the liquefaction resistance as shown in Fig. 3.7. For the same shear strain amplitude, the cumulative shear strain decreases as the phase difference increases. In Fig. 3.7, the curve of cumulative shear strain tends to converges to a value of G^* about 20%. This value of G^* means the minimum cumulative shear strain at which the liquefaction occurs and is considered as a criterion for the liquefaction resistance under multi-directional cyclic shear.

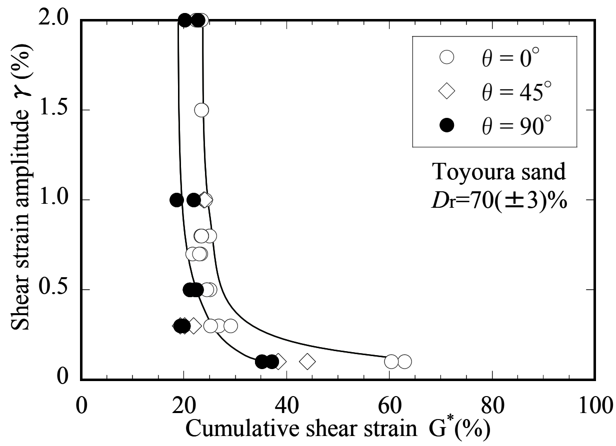

Figure 3.7. Relationship between the cumulative shear strain and shear strain amplitude required for liquefaction

3.3. Liquefaction under Earthquake-induced Shear Strain

Figs. 3.8(a) to (c) show records of shear strain waves when the shear strain-time histories were applied to the specimen for the acceleration time histories of Hyogo-ken Nanbu Earthquake 1995 in Fig. 1.18(a). The patterns of these records are almost similar to the original ones in Fig. 1.1(a). In Fig. 3.8(a), the shear strain amplitude of EW (γ_{EW}) and NS (γ_{NS}) directions is almost equal to that of the original record, while in Figs. 3.8(b) and (c), the shear strain amplitude were enlarged and applied to the specimen from the two perpendicular directions.

The relationships between stress reduction ratio induced by multi-directional irregular cyclic shear at different levels of shear strain amplitude and cumulative shear strain are shown in Fig. 3.9 for Toyoura sand. Despite of some scattering in the observed plots, it is observed that the reduction of vertical effective stress and the occurrence of liquefaction are almost similar for different levels of shear strain amplitude. The value of cumulative shear strain for liquefaction occurrence is at about G^* = 20% which is the same as the results in Fig. 3.7. Therefore, this result suggests that the process of liquefaction of soil specimen under irregular shear strain histories can be evaluated by the criterion for the liquefaction resistance derived from the relations between cumulative shear strain G^* and shear strain amplitude.

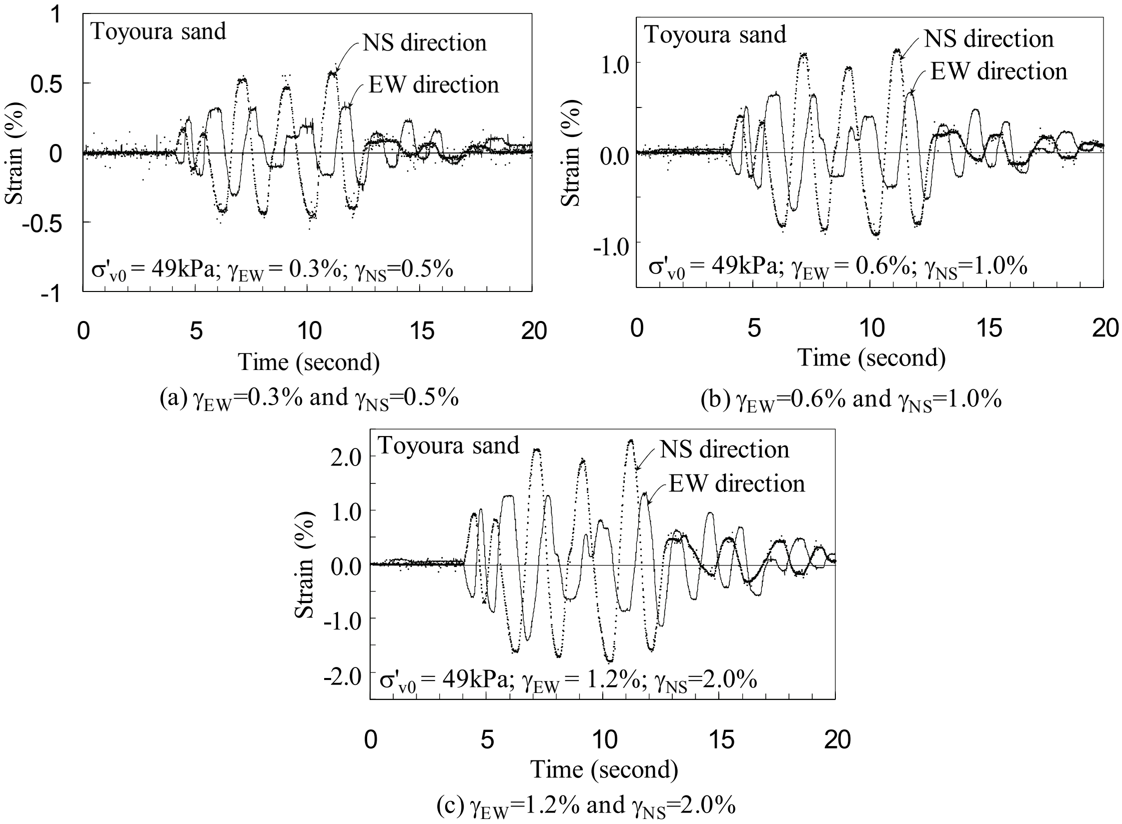

Figure 3.8. Time histories of shear strain in multi-directional irregular cyclic shear tests conducted for different scales of shear strain amplitude

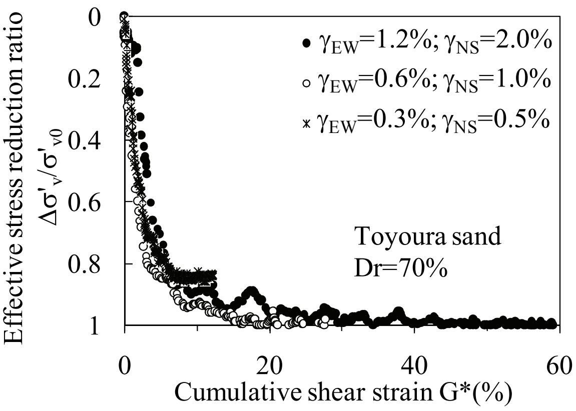

Figure 3.9. Relationships between stress reduction ratio and cumulative shear strain during multi-directional irregular cyclic shear tests performed for different scales of shear strain amplitude

4. CONCLUSIONS

In order to clarify the effect of cyclic shear direction on the liquefaction characteristics of saturated saturated granular materials, several series of cyclic simple shear test were carried out by using the multi-directional cyclic simple shear test apparatus. The main conclusions are summarized as follows:

1. For crushable and non-crushable granular materials subjected to multi-directional cyclic shear with various phase differences, the reduction of effective vertical stress can be evaluated by a function of cumulative shear strain G^*.

2. The relationships between cumulative shear strain and shear strain amplitude when the liquefaction occurs are possible to use as a criterion for the liquefaction resistance. The minimum value of cumulative shear strain required to reach liquefaction is of about 20%. The liquefaction of soil specimen under the irregular shear strain histories can be evaluated by this criterion.

ACKNOWLEDGEMENT
A part of this study was supported by Grant-in-Aid for Scientific Research (C), (23560993) and the experimental works were also supported by the students who graduated Yamaguchi University. The writers would like to express their gratitude to their supports.

REFERENCES

Fukutake, K. and Matsuoka, H. (1989). A unified law for dilatancy under multi-directional simple shearing. *Journal of JSCE Division C, JSCE* **412:III-1**,143-151. (in Japanese)

Ishihara, K. and Yoshimine, M. (1992). Evaluation of settlements in sand deposits following liquefaction during earthquakes. *Soils and Foundations* **32:1**,173-188.

JGS. (2000). Soil test procedure and explanation. (in Japanese)

Matsuda, H., Shinozaki, H., Okada, N., Takamiya, K. and Shinyama, K. (2004). Effects of multi-directional cyclic shear on the post-earthquake settlement of ground. *13th World Conference on Earthquake Engineering*. Paper No.2890.

Matsuda, H., Baek, W.J. and Shinyama, K. (2006). Effect of particle crushing on the geotechnical properties of GBFS. *Geomechanics and Geotechnics of Particulate Media*. Taylor and Francis Group, London.

Matsuda, H., Shinozaki, H., Ishikura, R. and Kitayama, N. (2008). Application of granulated blast furnace slag to the earthquake resistant earth structure as a geo-material. *14th World Conference on Earthquake Engineering*. Beijing, China.

Matsuda, H., Andre, P.H., Ishikura, R. and Kawahara, S. (2011). Effective stress change and post-earthquake settlement properties of granular materials subjected to multi-directional cyclic simple shear. *Soils and Foundations* **51:5**,873-884.

Pyke, R., Seed, H.B. and Chan, C.K. (1975). Settlement of sands under multidirectional shaking. *Journal of Geotechnical Engineering, ASCE* **101:GT4**,379-398.